International Journal of Radiology and Diagnostic Imaging

E-ISSN: 2664-4444
P-ISSN: 2664-4436
www.radiologypaper.com
IJRDI 2020; 3(4): 27-34
Received: 18-08-2020
Accepted: 22-09-2020

Dr. Hemalatha Sappidireddi
Senior Resident, Department of Radiodiagnosis, ESIC Medical College, Hyderabad, Telangana, India

Dr. Suneeth Jogi
Assistant Professor, Department of Radiodiagnosis, ESIC Medical College, Hyderabad, Telangana, India

Dr. Chinmayee Biswal
Senior Resident, Department of Radiodiagnosis, ESIC Medical College, Hyderabad, Telangana, India

Dr. Pavani Tummala
Consultant, Dept of Radiodiagnosis, Medicover Hospital, Hyderabad, Telangana, India

Corresponding Author:
Dr. Suneeth Jogi
Assistant Professor, Department of Radiodiagnosis, ESIC Medical College, Hyderabad, Telangana, India

Role of MRI in the evaluation of Sellar and Parasellar masses

Dr. Hemalatha Sappidireddi, Dr. Suneeth Jogi, Dr. Chinmayee Biswal and Dr. Pavani Tummala

DOI: http://dx.doi.org/10.33545/26644436.2020.v3.i4a.133

Abstract
Introduction: Sellar and parasellar/juxtasellar regions are sophisticated areas of the brain, and varied types of tumors can present in this area. Preoperative non-invasive diagnosis with magnetic resonance imaging (MRI) is essential for treatment planning.
Aim: The aim of this study is to characterize MRI features of the sellar and juxtasellar tumors and to correlate MRI diagnosis with histopathological diagnosis in order to evaluate the efficiency of MRI.
Materials and Methods: Patients with sellar and juxtasellar lesions who were operated during September 2017–May 2020 and the pathological reports were compared with the MRI findings retrospectively.
Results: 100 patients in total were enrolled for this study. Results were analysed and discussed.
Conclusions: The present study revealed a strong correlation between MRI and histopathological diagnosis for sellar and juxtasellar tumors. MRI is the modality of choice to distinguish and describe sellar- suprasellar lesions.

Keywords: MRI sellar lesions, MRI parasellar Lesions, MRI adenoma, Dural Tail Sign, Cavernous sinus invasion

Introduction

The sellar and para sellar region is an anatomically complex area and represents a crucial crossroad of critical neurovascular structures, e.g. orbits, cavernous sinus and its contents, supra sellar cistern and its contents, circle of Willis, hypothalamus through the pituitary stalk and dural reflections forming the diaphragm sellae and the walls of the cavernous sinuses. The cavernous sinus represents the most relevant parasellar structure, but from the practical and clinical point of view all the structures that surround the sella turcica are included in the parasellar region. The sellar and parasellar region anatomy is intricate, with diverse pathology [1] [Figure 1]. Various types of tumours, cysts, vascular lesions, inflammatory processes, infections and congenital lesions are found in and around the sella.The clinical presentation of the sellar and parasellar lesions is variable. Pituitary axis dysfunction, visual field defects, hydrocephalus, intracranial mass effect and other neurologic deficits are some of the most common features [3, 4].

Although different imaging modalities are used for assessment of this area, introduction and widespread use of high resolution computed tomography (CT) has relegated its imaging predecessors, such as plain skull roentgenograms, pleuridirectional tomography and pneumo-encephalography to obsolescence [2]. Magnetic resonance imaging (MRI) is now widely available, and considerable body of experience has been accumulated in using it to evaluate this region. MRI is now widely accepted as the imaging procedure of choice in the evaluation of sellar and parasellar pathology. Its major advantages are its superior soft tissue contrast and capacity for multiplanar imaging. Also there is no artefact from bone, and the patient is not exposed to ionizing radiation. Involvement of the optic chiasm, cavernous sinus, sphenoid sinus, orbit, temporal lobes and carotid arteries can all be best seen with MRI [5]. For evaluation of calcification and bone detail, CT is the preferred imaging modality. However, CT has its own drawbacks of high doses of ionizing radiation, artifacts due to presence of bony structures and inherent limitation of soft tissue resolution. But still CT remains important screening modality. Regardless of which imaging modality is used, it is useful to review the normal radiological anatomy and to survey the more common types of

pathologic entities that occur in it [6, 7, 8].

It is important to make an attempt to characterize the histological etiology of masses involving sellar, juxta sellar region. This is of profound clinical importance as this determines the use of surgical versus nonsurgical techniques, a transsphenoidal versus intracranial surgical approach and the degree of resection.

In present study, we have evaluated 100 patients, having referred with strong clinical suspicion or preliminary CT showing abnormality in the sellar, parasellar region.

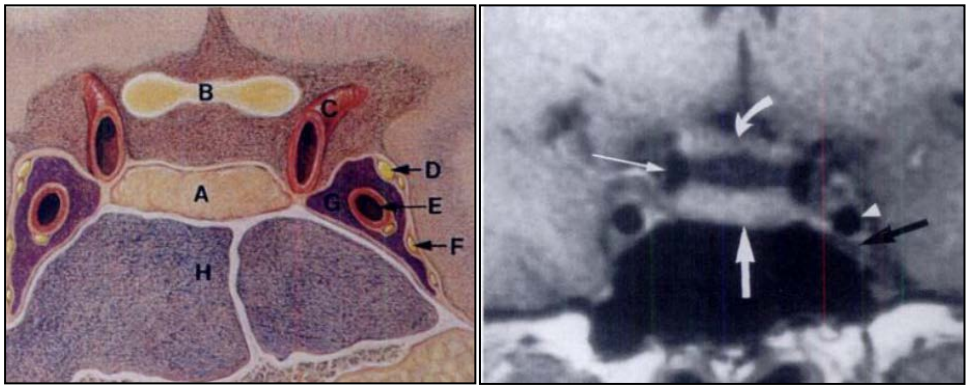

Fig 1: A) Drawing illustrate of normal anatomy of sellar and parasellar region in coronal plane. A-adenohypophysis, B-optic chiasm, C-supraclinoid ICA, D-oculomotor nerve, E-cavernous ICA, F-ophthalmic nerve, G-cavernous sinus, H-sphenoid sinus. B) Corresponding T1W coronal image showing adenohypophysis (thick white arrow), optic chiasm (curved white arrow), supraclinoid ICA (thin white arrow), cavernous ICA (arrowhead), cavernous sinus (thick black arrow).

Methodology

The present Study included 100 patients with clinical features raising suspicion of sellar and parasellar lesions, hormonal alterations pointing towards pituitary pathology and also the patients who have been diagnosed as having sellar and parasellar lesions on CT SCAN and needed further evaluation with MRI at our institute. The patients having contraindications to MRI such as: Aneurysmal clips;Cardiac pacemaker; Implanted cardiac defibrillator; Neurostimulation system; Spinal cord stimulator; Cochlear, otologic or other ear implant were excluded from the study.

The study was performed with Philips Ingenia 1.5 Tesla MRI machine. Brain screening sequences used were T2W and FLAIR axial sequences.

After this, high resolution T1SE and T2SE sequences focused on the sellar region are performed in all cases. T1FS postcontrast axial sequence is also performed in all cases using Gadolinium DTPA. In cases of pituitary microadenoma, the rapid dynamic postcontrast scan is done. MR angiography using 3D TOF sequence was done in cases where vascular pathology suspected. In addition Diffusion sequence was taken wherever thought essential, like in cases of epidermoid cysts.

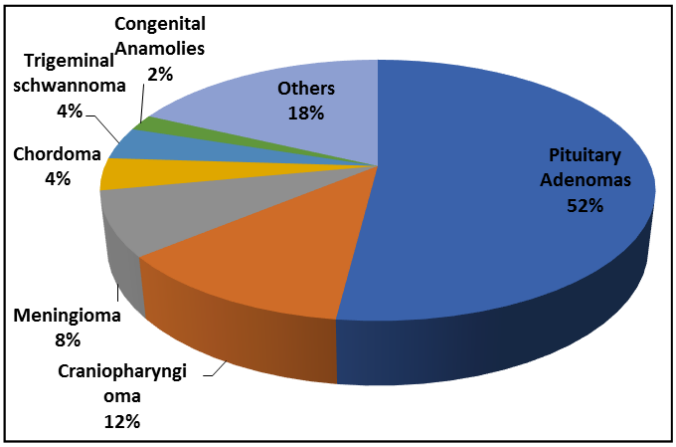

Fig 2: Distribution of pathologies in Sellar and Parasellar region

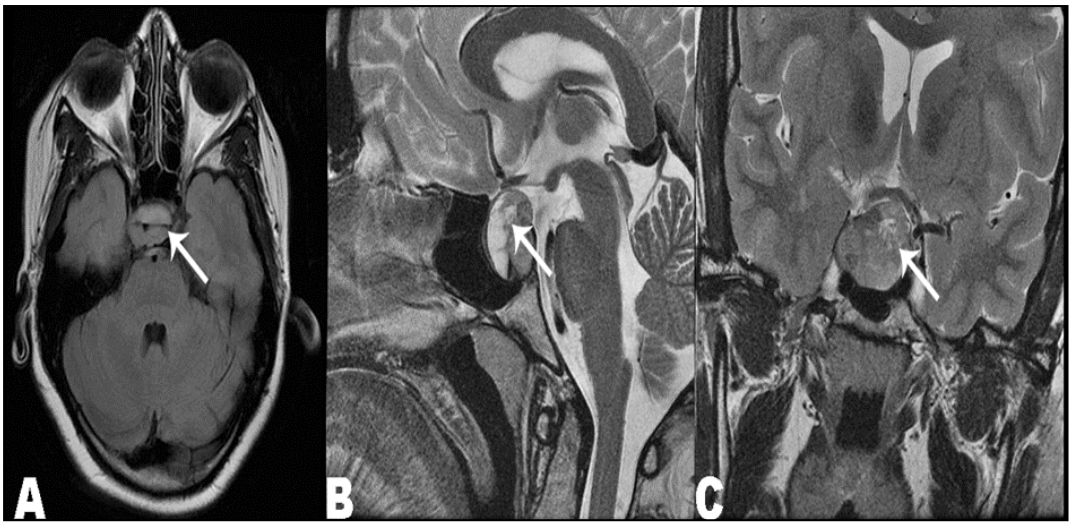

Fig 3: Pituitary apoplexy Figure A, B, C: Axial FLAIR, Sag T2 and Cor T2 images respectively showing illdefined heterogenous lesion with fluid-fluid levels representing hemorrhage within a solid mass in pituitary fossa extending into suprasellar region. Pituitary macroadenoma with hemorrhage was considered as diagnosis.

Results

A total of 100 cases with sellar and parasellar pathologies were reviewed during 2017-2020, of which 36% were males (n=36) and 64% were females (n=64).

Pituitary adenomas were found to 52% of the case series. Other diagnosis noted are documented in Table 1.

Adenomas were commonly seen in females (62%) and mostly in the age group range of 31-40 (43%). Microadenomas (53.4%) were more in frequency than Macroadenomas (46.15%). The Table 2 are the specific clinical features with height and cavernous sinus extension in cases of macroadenomas.

Histopathologically, the microadenomas in the series were classified further. Prolactinomas (10%) of total tumours of sellar and parasellar regions. MRI characteristics of adenomas are tabulated as follows in the Table 3.

Morphologically, Solid lesions are predominant in Macroadenomas (85.7) and Meningioma (100%) and Mixed lesions are common in Craniopharyngioma (83.3%) and their features are described in Table /Figure 5.

Calcification, Bony erosions, Hydrocephalus, Peritumoral oedema are commonly observed associated features in sellar lesions. Calcifications and Hydrocephalus are more common among craniopharyngiomas (66.6%).

Bony erosions are commonly seen in 35.7% of macroadenomas. Dural Tail sign is seen in 75% of Meningioma. Bony Hyperostosis is also seen in 50% 0f Meningiomas.

Table 1: Clinical features with height and cavernous sinus extension in cases of macroadenomas

S No	Clinical feature	Percentage in case series	Avg height	Cavernous sinus extension	surgically proven invasion
1	Chiasmal syndrome	78.6%	2.4 cm	5	4
2	Amenorrhoea and galactorrhoea or decreased libido	42.8%	2.5 cm	0	0
3	Acromegaly	14%	2.2 cm	1	1
4	Hypopituitarism	14%	2.9 cm	1	1

Table 2: MRI characteristics of Microadenomas

Microadenoma(n=12)	T1 signal intensity	T2 signal intensity	Dynamic enhancement	Average size	Convexity of superior margin of pituitary
Prolactinomas (n=8)	Iso/Hypo	Iso to Hyper	Seen after 100-120 sec	7mm	8
GH secreting microadenoma (n=1)	Iso/Hypo	Hyper	Seen after 100-120 sec	5mm	1
ACTH secreting microadenoma(n=1)	Iso/Hypo	Hyper	Seen after 100-120 sec	3mm	0

Table 3: MRI Characteristics of lesions in sellar and parasellar regions

T1W signal intensity characteristics			
T1W signal intensity	**Macroadenoma**	**Meningioma**	**Epidermoid cyst**
Isointense	57.1%	75%	0
Hypointense	35.7%	0	100
Hyperintense	7.14%	25%	0
T2W signal intensity characteristics			
T2W signal intensity	**Macroadenoma**	**Meningioma**	**Epidermoid cyst**
Isointense	35.7%	100%	0
Hypointense	7.1%	0	0
Hyperintense	57.1	25%	100%
T1W Lesion in homogenesity Characteristics			
T1W Lesion inhomogenesity	**Macroadenoma**	**Craniopharyngioma**	**Meningioma**
None	21.4	_	50%
Mild	57.1%	16.6%	50%
Moderate	14.2%	66.6%	_
Marked	7.1%	16.6%	_
T1W Lesion in homogenesity Characteristics			
T2W Lesion inhomogenesity	**Macroadenoma**	**Craniopharyngioma**	**Meningioma**
None	7.1%	_	50%
Mild	14.2%	_	50%
Moderate	42.8%	33.3%	_
Marked	35.7%	66.6%	_
Enhancement pattern of common sellar lesions			
Pattern enhancement	**Macroadenoma**	**Craniopharyngioma**	**Meningioma**
None	0	0	0
Homogenous	71.4%	0	100%
Heterogenous	28.57%	83.3%	0
Peripheral	0	16.6%	0

Discussion

The present study was undertaken with an aim to evaluate MRI findings in sellar&parasellar lesions; in assessing diagnostic accuracy of MRI in characterization and histological typing of sellar and parasellar lesions.

The most common lesion detected in the present study was pituitary adenoma (26 out of 50) which was similar to the experience of Johnsen *et al.* [9]. In the present study, 26

pituitary adenomas were detected which constituted to about 52% of total pathologies in sellar and parasellar regions. Out of 26 adenomas 14 were macroadenomas and 12 were microadenomas by size criterion. So the proportion was about 1.1:1. Johnsen *et al.* [9] found the total proportion of macro to microadenomas 2.5:1.

Macroadenoma [Figure 4]: Patients with macroadenomas presented with symptoms of mass effect rather than endocrinological disturbances. In our study about 78.6% patients presented with symptoms of visual disturbances while 53% of macroadenomas were having endocrinological disturbances. The average height of macroadenomas producing visual disturbances found to be 2.4 cm. 57.1% of macroadenomas were of medium size (2 to 4cm) at the time of scanning. This explained the larger no. of patients presenting with visual disturbances. In the study by Johnsen *et al.* [9] also visual disturbances were found to be the most common complaints with macroadenomas with average height being 2.7cm.The microadenomas being too small to create any mass effect, the patients presented usually with signs and symptoms of hormone excess. The most common type of microadenoma detected in our study was prolactinoma (83%) which was consistent with the literature.On T1W images (60%) of macroadenomas were isointense to grey matter, 34% were hypointense and 6% were hyperintense. The hyperintensity on T1WI in 6% cases was found to be due to presence of pituitary apoplexy [Table/Figure 6]. Out of 51 cases studied by Johnsen *et al.* [9], he found about 82% lesions were isointense to grey matter. On T2W images the macroadenomas showed variable signal intensity depending upon their composition. After the contrast administration, 22 cases (69%) showed homogenous enhancement on postcontrast study while 10 cases (31%) showed heterogeneous enhancement. Johnsen *et al.* [9] found homogenous enhancement in 46% cases.

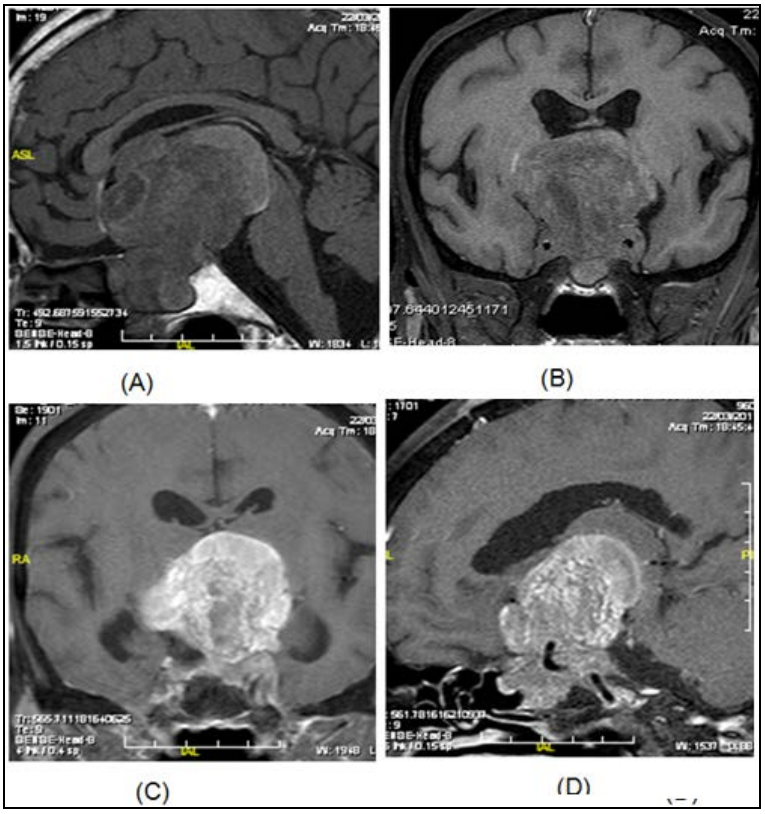

Fig 4: Large macroadenoma A) T1W sagittal and B) T1W coronal images showing a large mixed signal intensity mass in sellar and suprasellar region causing compression and superior displacement of chiasm, hypothalamus, thalamus and third ventricle. Pituitary not visualised separatly. Encasement of cavernous portion of bilateral ICA'S noted. (C) and (D) are the post contrast T1W coronal and sagittal images respectively show heterogenous enhancement with non-enhancing areas in the centre of the lesion s/o necrotic changes.

Cavernous sinus invasion

There were 5 cases of surgically proven cavernous sinus invasion. The most specific sign for the detection of cavernous sinus invasion was total encasement of the internal carotid artery. It has got 100% specificity with 100% positive predictive value. However, it has got very low sensitivity and negative predictive value of 33.33% and 60% respectively. So, cavernous sinus invasion evaluation by this sign is useful only in advanced cases. Scotti *et al.* [10] found, this sign to be the most specific for detection of cavernous sinus invasion. Asymmetric lateral bulge of the lateral wall of the cavernous sinuses was found to be the most sensitive sign to detect cavernous sinus invasion. This has got 83.33% sensitivity, 83.33% positive predictive value and 66.66% specificity

Microadenoma: While during dynamic postcontrast imaging, the lesions started enhancing after 100 to 120 seconds and reached at peak during 180-200 seconds. The normal pituitary started enhancing after 40 to 60 seconds with peak enhancement during 100 to 120 seconds. The average time for optimal tumour delineation was about 90 sec. These findings were similar to the, larger study performed by Kasaliwal *et al.* [11], for dynamic postcontrast evaluation of microadenomas. While all lesions were visible on precontrast high resolution images, the dynamic postcontrast study made the lesions more conspicuous, increasing the confidence.

Craniopharyngioma [Figure 5]: In the present study, there were 13% patients of suprasellar craniopharyngiomas. Johnsen *et al.* [9] in their retrospective study noted 10 (7.6%) cases of craniopharyngioma out of 131 cases.In solid-cystic cases cystic component is iso to hyper on T1W & T2W images. Solid component is iso to hypo on T1W Isointense on T2W images. Solid lesions show mixed signal intensity on T1W & T2W images. On post contrast study cystic component show peripheral enhancement and solid portion show heterogenous enhancement.

The wide range of histologic appearances of craniopharyngiomas was reflected in their MR appearances. Although definitive statements concerning calcium and cholesterol content cannot be made without complete sectioning of the entire specimen, qualitative examination of the sections correlated well with the several MR patterns. High intensity on T1weighted images was noted in cystic lesions with high cholesterol content or containing methemoglobin. Kjos *et al.* [12] described high-intensity signal on T1-weighted images of hemorrhagic Cysts. Bradley and Schmidt [13] showed that Methemoglobin formation with T1 shortening at least partially accounts for the increasing MR signal intensity of subarachnoid hemorrhage with time. Moderate intensity on T1 weighted images was noted in tumours lacking significant cholesterol or blood. Both these groups demonstrated high signal intensity on T2-weighted images.

The presence of calcification is noted in (53%) cases. In a study by Hirunpat *et al.* (14 which compared the CT and MRI in assessment of craniopharyngiomas, they found that, CT was superior to MR in demonstrating calcifications within the tumours. MR failed to demonstrate areas of calcification in three of 14 cases in which calcification was demonstrated by CT. In one case, calcification would have been incorrectly suspected on the basis of MR. Johnsen *et al.* [9] also concluded that, CT provides superior demonstration of tumoural calcification and, hence, may permit a more specific diagnosis when this common characteristic is demonstrated. This is a circumstance in which CT assumes a particularly useful role as a diagnostic adjunct.

Although all were primarily suprasellar in location, all cases of craniopharyngiomas in our study showed intrasellar extension. Bony sellar wall erosion is seen is seen in 23% of cases. The sellar expansion was not as large as in pituitary adenomas. Only one case showed significant sellar expansion. Sartor *et al.* [5] showed bony sellar wall erosion in 44% of cases of craniopharyngiomas**.** Jiang *et al.* [15] further stated that, if mass is centered in the sella with significant sellar expansion and bony erosion, the possibility of pituitary adenoma is likely. Our study also supported this hypothesis In this study, we found craniopharyngioma to be the most common tumour in sellar & parasellar region to be associated with hydrocephalus (53% cases). This is related to the fact that the craniopharyngiomas tend to grow larger in size and cause more mass effect than any other lesion. Superior, lateral, posterior and inferior extensions of craniopharyngiomas are better demonstrated in contrast enhanced coronal sequences as in pituitary macroadenomas.

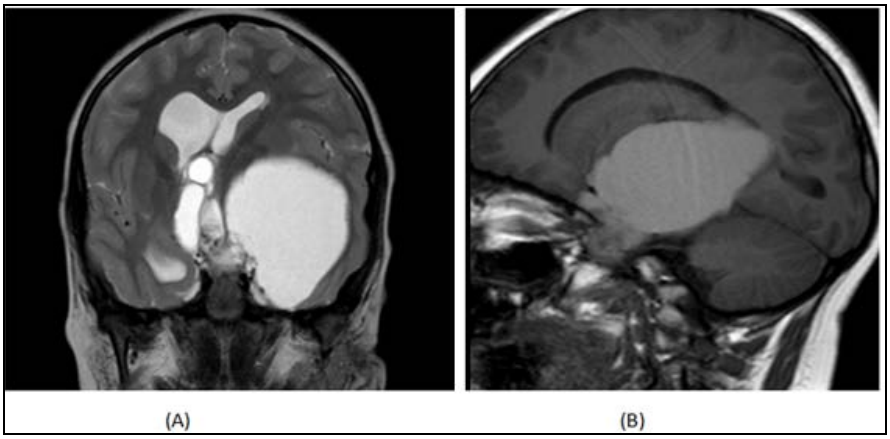

Fig 5: Craniopharyngioma: A) T2W coronal and B) T1W sagittal images showing a large solid-cystic lesion in sellar, supra and parasellar region. Cystic component is hyperintense on T1W and T2W images. solid component is iso to hypointense on T1W and hyperintense on T2W images. Mass effect in the form of effacement of left lateral, third ventricle and mild midline shift is noted.

Meningiomas [Figure 6]

Meningiomas in sellar region may arise from tuberculum sellae, diaphragma sellae, clinoid processes, optic nerve sheaths and wings of sphenoid. Meningiomas in parasellar region may extend in to the sellar region.

Isointensity on T 1- and T2-weighted images is a characteristic signal intensity feature of meningiomas. With over 50% being isointense to cortex on TI- and T2-weighted images, but similar findings in macroadenomas make this feature of little use in differentiation. In our study, we found 7 out of 10 (70%) meningiomas to be isointense on T1W and T2W images. Atypical features such as presence of hemorrhage and cystic components have also been described in literature. Taylor *et al.* [16] found that 91% of meningiomas were isointense on T1 and 55% were isointense on T2W. In contrast, 79% of macroadenomas were isointense on T1W, while only 32% of macroadenomas showed Isointensity on T2W.This led to finding that T2W signal intensity may be an important point to distinguish between the adenoma and meningioma.

Fatty marrow which is hyperintense on T1 weighted imaging points towards hyperostosis which is seen as focally expanded bone. Thick cortical bone will not produce any signal and is therefore as easily recognizable. In our study, hyperostosis was present in 2 cases of meningiomas. Hyperostosis is a commonly encountered feature of meningiomas in any location and has been reported in 34% of meningiomas involving the sella. Hyperostosis may sometimes be seen in metastases and may rarely be mimicked by dense calcification associated with

craniopharyngiomas and aneurysms, but true osseous thickening still remains highly specific for meningioma. Dural tail enhancement or the meningeal sign is commonly associated with meningiomas but is not entirely specific. In our study (50%) out of 10 cases showed dural tail sign. No other tumour showed this sign.

Of the ten patients of meningioma 9 were correctly diagnosed. In one case, the tumour was primarily located in sella and showed suprasellar and parasellar extension. No hyperostosis, Peritumoural calcification is seen. It had a few foci of cystic degeneration. This turned out to be pituitary adenoma. Such types of mimicking between meningiomas the pituitary adenomas are described in literature and needs careful evalution of clinical picture, neuroimaging and endocrine studies [17].

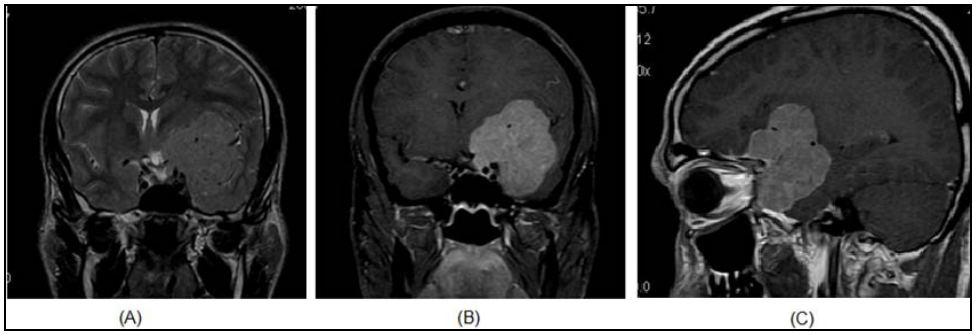

Fig 6: Parasellar meningioma A) T2W coranal image showing isointense extraaxial mass in left parasellar region involving left cavernous sinus. B) and C) are post contrast T1W coronal and sagittal images respectively show homogenous enhancement of the lesion.

Epidermoid cyst [Figure 7]

There were total 5 (5%) epidermoid cysts out of 100 cases. They were arising in suprasellar &parasellar region. One was of medium size and other three were of larger size. In our study, we found epidermoids as slightly hyperintense to CSF on T1W & T2W images and showed bright signal on diffusion. There was no enhancement on post contrast study.All epidermoid cysts relatively followed CSF signal intensity on T1W and T2W. All cases showed incomplete suppression on FLAIR and bright signal on Diffusion**.** Hakymayez *et al.* [18] evaluated role of FLAIR and diffusion weighted imaging in differentiating the epidermoid and arachnoid cysts. They found that FLAIR sequence was clearly superior to conventional T1 and T2W images for differentiation. All epidermoid cysts were hyperintense on diffusion with mean ADC value was more than arachnoid cysts but higher than cerebral cortical white matter. This finding also suggests that epidermoid cysts are not truly 'restricted' on DWI rather they show 'shine through' effect owing to their high mean ADC values. No post contrast enhancement is seen in all cases.

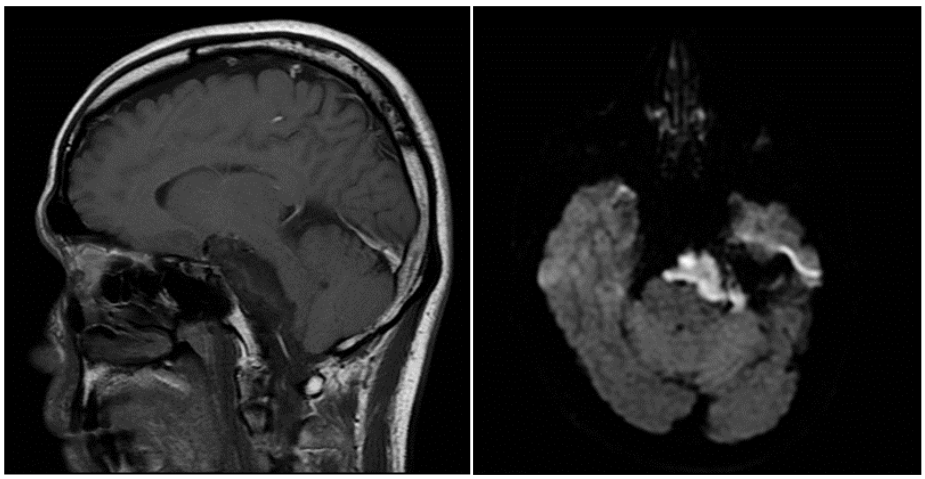

Fig 7: Epidermoid cyst A) T1W sagittal and B) DWI axial images showing ill-defined cystic mass encasing the basilar artery in supra and parasellar region mildly hyperintense to CSF on T1W images and bright on DWI sequence

Trigeminal schwannoma

The fifth cranial nerve is the second most common site of intracranial neuroma and the most frequent cranial nerve tumour to cause parasellarmass. In our study we found three cases of trigeminal schwannoma in adult patients. They were isointense to brain on T1W and hyperintense on T2W images. Intense enhancement noted on postcontrast study. They follow the course of nerve.

Chordoma

Two cases of the chordoma were detected in sellar and parasellar region. All cases were adult. One was female and three were male. On T1W, they were iso to hypointense. On T2W images heterogeneous high signal intensity with hypointense septations noted. On postcontrast study, strong heterogeneous enhancement is seen in all cases. There was gross bony destruction seen in two cases. Our findings are also comparable with the larger series study on chordoma by Sze G *et al.* [19].

Hypothalamic hamartoma

There were two cases of hypothalamic hamartomas

presented with features of precocious puberty. They were isointense on T1W, slightly hyperintense on T2W and showed no enhancement on postcontrast study.

Arita *et al.* [20] have shown that para hypothalamic hamartomas are more commonly associated with precocious puberty than an intrahypothalamic glioma which was associated with gelastic seizures. This was isointense on T1W, slightly hyperintense on T2W and showed no enhancement on postcontrast study. Also in literature it has been stated that, the absence of any long-term change in the size, shape, or signalintensity of the lesion strongly supports the diagnosis of hypothalamic hamartomas.

Lymphocytic hypophysitis

There was one case of Lymphocytic hypophysitis. A peripartum female presented with symptoms of headache, lactational failure, failure to resume menses and visual loss. MR demonstrated diffuse enlargement of anterior lobe and there was no evidence of focal abnormality. Thickening of pituitary stalk noted. Loss of posterior pituitary hyperintense signal is noted.Nakata *et al.* [21] retrospectively reviewed the MR imaging findings in 20 patients and concluded that MR findings such as loss of posterior pituitary bright spot, thickened stalk, pituitary asymmetry, homogenous enhancement and parasellar T2 dark sign can contribute to distinguishing pituitary adenoma from Lymphocytic hypophysitis.

Rathke cleft cyst

There was one case of Rathke cleft cyst in our study. Female patient, presented with headache and visual disturbances and with signs of hypopiyuitarism.MRI revealed cystic lesions in sellar and suprasellar region iso to hyperintense on T1W and hyperintense on T2W images. No enhancement noted on postcontrast study. Kunii *et al.* [21] found two cases in their study both of them young girls presented with headache and seizures.

Arachnoid cyst

There was one female patient of arachnoid cyst in our study who presented with seizures, headache and visual disturbances. The lesion was Homogenous and well marginated in suprasellar area that followed CSF signal intensity on all pulse sequences [22].

Suprasellar tuberculomas

This was a 23 year female who presented with convulsions headache and visual disturbances. There were multiple conglomerated ring enhancing lesions seen in the optic chiasma, tuber cinerium and pituitary stalk. Most were isointense on T1WI and few were hypointense. On T2W images they were predominantly hypointense with few being hyperintense. Pituitary tuberculomas are rare, though they were not an uncommon finding in autopsy material reported in the early half of this century. In a review of reported cases of intrasellar tuberculoma, Taylor *et al.* [16] found that most have headache as the presenting complaint in addition to visual disturbances. Thus, in the present study, MRI was very usefull in prediction of tumour pathology in cases of sellar and juxtasellar masses. Following features that were highly suggestive for predicting tumour pathology were noted: a) Sellar wall erosion in a mass which was associated with significant sellar expansion and centered in sella in case of pituitary macroadenoma. b) Solid cystic lesion with prominent cystic component and presence of calcifications within in a child highly favors diagnosis of craniopharyngioma. This also showed most variable signal intensity pattern. c) Tumour in an adult female, which is making an obtuse angle with dura, homogeneous, isointense signal on T1W and T2W and strong bright homogenous enhancement on postcontrast study, favors the diagnosis of meningioma. In addition to this, it also shows presence of hyperostosis and 'dural tail' sign which significantly aids in diagnosis.

Acquired Empty sella [Figure 8]

One case of empty sella was detected. Female of childbearing age presented with symptoms of pituitary hormonal deficiencies such as secondary amenorrhea, weght loss, lactational failure & headache. She history of circulatory collapse during peripartum period. MR done between 6 month postpartum revealed marked atrophy of pituitary gland resulting in empty sella.

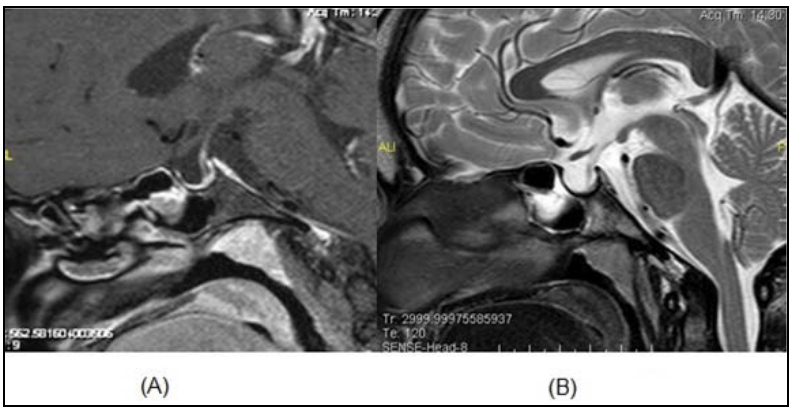

Fig 8: Acquired empty sella: A) T1W sagital and B) T2W sagittal images showing sella filled with CSF with thin rim pituitary tissue along sella flour in six month post partum patient presented with hypopituitarism represent an empty sella syndrome.

Conclusion

Hence, finally to conclude, the MR imaging characteristics of the four most common lesions were sufficiently distinct to allow them to be differentiated from each other and from most other entities. Various other imaging features like enhancement post contrast, presence of cystic components, extrasellar and intrasellar location, and clinical symptoms permit further differentiation among the various other abnormalities. The superior resolution and multiplanar capacity of MR imaging best depicts the extent of sellar and parasellar lesions.

References

1. Anna Derman MD, Marisa Shields, Adam Davis MD, Edmond Knopp MD, Girish M Fatterpekar MBBS. Diseases of the Sella and Parasellar Region: An Overview. Seminars in roentgenology 2013, 35-50.
2. Swartz JD, Russell KB, Basile BA, O'Donnell PC, Poply GL. High resolution computed tomographic appearance of the intrasellar content in women of childbearing age. Radiology 1983;147:115-117.
3. De Herder WW. The History of Acromegaly. Vol. 103, Neuroendocrinology 2016, p. 7-17.
4. Herder WW. Acromegaly and gigantism in the medical literature. Case descriptions in the era before and the early years after the initial publication of Pierre Marie (1886). Pituitary 2009;12(3):236-44.
5. Sartor K, Karnaze MG, Winthrop JD, Gado M, Hodges FJ. MR imaging in infra-, para- and retrosellar mass lesions. Neuroradiology 1987;29(1):19-29.
6. Lee BCP, Kneeland JB, Walker RW, Posner JB, Cahill PT, Deck MD, *et al.* MR imaging of brainstem tumors. Am J Neuroradiol 1985;6(2):159-63.
7. Davis PC, Hoffman JC, Malko JA, Tindall GT, Takei Y, Avruch L, *et al.* Gadolinium-DTPA and MR imaging of pituitary adenoma: a preliminary report. Am J Neuroradiol. 1987;8(5):8170-23.
8. Brauner R, Argyropoulou M, Perignon F, Rappaport R, Brunelle F. [Role of magnetic resonance imaging in non-neoplastic hypothalamo-hypophyseal pathology]. Ann Pediatr (Paris) 1993;40(7):469-74.
9. Johnsen DE, Woodruff WW, Allen IS, Cera PJ, Funkhouser GR, Coleman LL *et al.* MR imaging of the sellar and juxtasellar regions. Radiographics 1991;11(5):727-58.
10. Scotti G, Yu CY, Dillon WP, Norman D, Colombo N, Newton TH, *et al.* MR imaging of cavernous sinus involvement by pituitary adenomas. Vol. 9, American Journal of Neuroradiology 1988, p. 657-64.
11. Kasaliwal R, Sankhe SS, Lila AR, Budyal SR, Jagtap VS, Sarathi V, *et al.* Volume interpolated 3D-spoiled gradient echo sequence is better than dynamic contrast spin echo sequence for MRI detection of corticotropin secreting pituitary microadenomas. Clin Endocrinol (Oxf) 2013;78(6):825-30.
12. Kjos B, Brant-Zawadzki M, Kucharczyk W, *et al.* Cystic intracranial lesions: magnetic resonance imaging. Radiology 1985;155:363-369.
13. Bradley G, Schmidt PG Ph.D. Effect of Methemoglobin on the MR Appearance of Subarachnoid hemorrhage. Radiology 1985;156:99-103.
14. Hirunpat S, Tanomkiat W, Sriprung H, *et al.* Optic tract edema: a highly specific magnetic resonance imaging finding for the diagnosis of craniopharyngiomas. Acta Radiol 2005;46:419-423.
15. Jiang X, Yang W. Analysis of MRI for tumor of the sellar region]. Yan Ke Xue Bao 2001;17(4):224-8.
16. Taylor SL, Barakos JA, Harsh GR, Wilson CB. Magnetic resonance imaging of tuberculum sellae meningiomas: preventing preoperative misdiagnosis as pituitary macroadenoma.Neurosurgery 1992;31:621-7.
17. Wolpert SM, Osborne M, Anderson M, *et al.* The bright pituitary gland: a normal MR appearance in infancy. AJNR Am J Neuroradiol 1988;9:1-3.
18. Hakyemez B, Aksoy U, Yildiz H, Ergin N. Intracranial epidermoid cysts: Diffusion-weighted, FLAIR and conventional MR findings. Eur J Radiol. 2005;54(2):214-20.
19. Sze G, Uichanco LS, Brant-Zawadzki MN, *et al.* Chordomas: MR imaging. Radiology 1988;166:187-191.
20. Nakata Y, Sato N, Masumoto T, Mori H, Akai H, Nobusawa H, *et al.* Parasellar T2 dark sign on MR imaging in patients with lymphocytic hypophysitis. Am J Neuroradiol 2010;31(10):1944-50.
21. Kunii N, Abe T, Kawamo M, Tanioka D, Izumiyama H, Moritani T, *et al.* Rathke's cleft cysts: Differentiation from other cystic lesions in the pituitary fossa by use of single-shot fast spin-echo diffusion-weighted MR imaging. Acta Neurochir (Wien) 2007;149(8):759-69.
22. Wiener SN, Pearlstein AE, Eiber A. MR imaging of intracranial arachnoid cysts. J Comput Assist Tomogr 1987;11:236-241.